A Low Out-of-Band Noise LTE Transmitter with Current-Mode Approach

Nicola Codega[1], Antonio Liscidini[2] and Rinaldo Castello[1]
[1]University of Pavia, Pavia, Italy [2]University of Toronto, Toronto ON, Canada
nicola.codega@unipv.it, antonio.liscidini@utoronto.ca, rinaldo.castello@unipv.it

***Abstract* — A 55nm CMOS current-mode transmitter for multistandard wireless communications (including LTE) that requires only 1.5mm^2 (with 4 output ports) is presented. The circuit is made up of two portions: a class A/B up-converter and a baseband that includes DAC, VGA, low-pass filter (two Biquad plus a passive first order) and class A/B signal conditioner. Combining a third order filter with the class A/B conditioner results in a reduction of both current consumption and RX-band noise injection. For LTE10, the consumption is 96mW and 34mW at 4dBm and at -10dBm output power, respectively. The complete transmitter gives -158dBc/Hz RX-band noise injection at 30MHz offset.**

I. INTRODUCTION

In direct-up transmitter architectures, the baseband signal can be up-converted to the RF by using either voltage or current mixers. In the first case, the most promising approach operates in the voltage-mode and is implemented with a quadrature passive up-converter driven by a filtering stage, followed by pre-power amplifier (PPA) [1], [2]. In the second case, the most efficient solution is based on a current power mixer, where the up-converter has also the role of a pre-power amplifier [3-5].

When a voltage passive mixer is adopted, the input capacitance of the PPA appears as a switched-capacitor (SC) load [1], [2], [6]. This increases the area and power consumption of the baseband (BB) since such load can be driven only lowering the output impedance of the last stage of the BB to reduce I and Q interaction. Furthermore, the mixer's switches must bear a large voltage swing without introducing non-linearity or degrading EVM.

Current-mode transmitter solutions are immune from SC loading and I and Q cross-talk. However, since the BB section generally still operates in voltage-mode, an additional linear V-I conversion stage is needed to drive the current-mode mixer [4], [5]. This makes voltage and current-mode solutions comparable in terms of power/area cost.

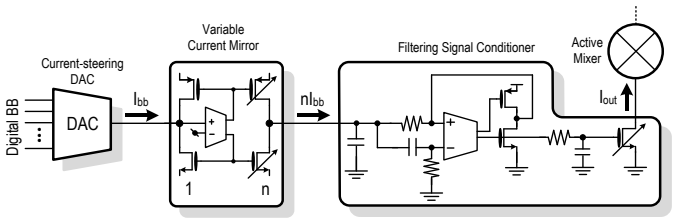

Fig. 1. Full current-mode class A/B transmitter

In this paper, we present a transmitter where the signal can be completely processed in the current domain from the DAC to the mixer output (Fig. 1). The transmitter is an evolution of the one reported in [4], where the filter used to minimize out-of-band noise and to remove DAC replicas is merged with the mirror stage that drives the class A/B power mixer. The result is a TX chain with high efficiency and lower RX-band noise (especially for narrow spacing) compared to the state of the art of 4G cellular transmitters.

II. CURRENT-MODE TRANSMITTER

A conceptual block diagram of the proposed transmitter is shown in Fig. 1. The output signal provided by a current-steering DAC is buffered, scaled up and sent to a current-driven third order filter that provides the class A/B output current to the power mixer. Compared to the solution reported in [4], the wideband V-I converter at the end of the TX chain is transformed in a current-driven filtering stage.

Moving the filter in the last building block of the BB chain not only potentially reduces power consumption (having merged two blocks into a single one) but also provides sharper filtering for the out-of-band noise of the BB. This becomes crucial in SAW-less applications when the TX-band and RX-band spacing is narrow and the signal channel large (e.g. LTE10 Band17, LTE20 Band20).

978-1-4799-0645-1/13/$31.00 ©2013 IEEE

A. Class A/B Variable Current Mirror

The first stage of the TX chain is a variable-gain current mirror that buffers the DAC output (Fig. 1). The mirror, operated in class A/B for better power efficiency, minimizes the voltage swing at the output of the DAC to increase its linearity, has a large output impedance to drive the following stage in current and allows gain control.

A two-stage class A/B OTA [7] drives the gates of a push-pull stage, realizing a boosted diode connection where the input impedance is lowered by a factor equal to the loop gain. The input current is then mirrored to the output through a scaled replica of the input branch.

B. Filtering class A/B signal conditioner

The core of the transmitter is the filtering signal conditioner that drives the power mixer in class A/B (Fig. 1). This block derives from the V-I converter (Fig. 2-a) proposed in [4]. The converted current is absorbed by the OTA output stage and fed to the mixer in a way that corresponds to an N-only class A/B transconductor [4].

The proposed current-mode TX chain, on the contrary, does not need any V-I converter, while the N-only class A/B transconductor is still necessary. The OTA is then used to implement an active inductor (Fig. 2-b) that creates a second order low-pass transfer function.

The inductive behavior is obtained creating a high-pass virtual short between the terminals of the input resistor R_1. This reduces the high-frequency components of the current absorbed by the OTA. The virtual short is realized adding a high pass filter (C_2R_2) between the terminals V_{in} and the inverting input V_- of the OTA (Fig. 2-b). At low frequency all the input current is absorbed by the OTA (neglecting C_1 for the moment) since C_2 is an open circuit and terminal V_+ is virtually shorted to ground. On the contrary, above the cut-off frequency $1/R_2C_2$, V_+ becomes equal to V_{in} and the two terminals of the resistor are virtually shorted preventing any flows of current into the OTA. A capacitor C_1 is then added at the input, leading to a second order filtering profile with an in-band gain of one, and ω_0 and Q given by

$$\omega_0 = \frac{1}{\sqrt{R_1C_1}\sqrt{R_2C_2}}\ , \qquad (1)$$

$$Q = \frac{\sqrt{R_2C_2C_1}}{\sqrt{R_1}(C_1+C_2)} \approx \frac{\sqrt{R_2C_2}}{\sqrt{R_1C_1}} \quad (\text{if } C_1 \gg C_2). \qquad (2)$$

To manage multiple wireless standards using the same architecture, the ω_0 must be reconfigurable. Its value should be as close as possible to the signal bandwidth (in trading-off with EVM, area and linearity) to perform the maximum filtering. Equations (1) and (2) show that it is possible to change ω_0 without changing the Q factor (i.e. maintaining the same filter shape).

Moreover, ω_0 and Q are not affected by the signal level since they are only a function of passive elements. In [8], a similar current-mode approach in the BB filtering was proposed for 3G standard, but the filter parameters were related to MOS transconductance (g_m) values. Since, to improve the signal-to-noise ratio (SNR), the swing is usually maximized, the g_m varies substantially with the signal level.

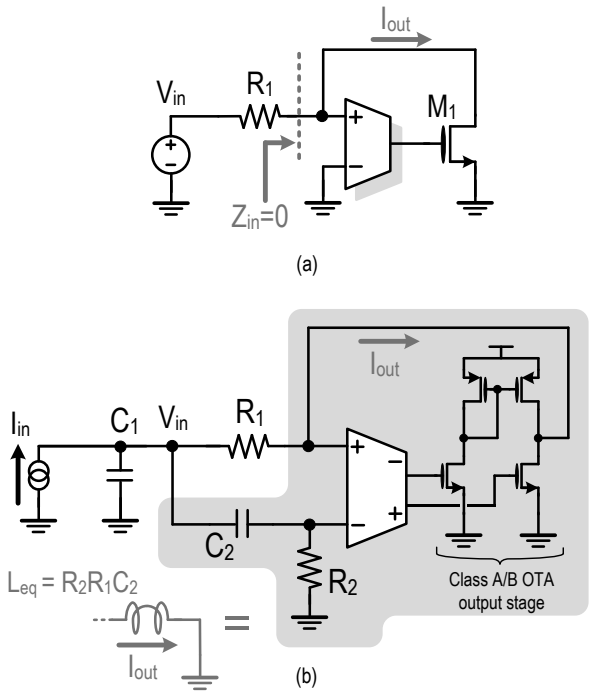

Fig. 2. (a) V-I converter in [4] (single-ended version);
(b) proposed filtering class A/B signal conditioner (single-ended version)

Time-variance of g_m makes the filter signal-dependent causing distortion and degrading the EVM.

C. Noise

While in a receiver the filters should be placed at the beginning of the analog chain to eliminate the interferers, in a transmitter the filtering should be done at the end of the BB to minimize its out-of-band noise and non-linearities. This is easily implementable in a voltage-mode transmitter [1], [2] and it was also proposed for the 3G current-mode transmitter in [8].

However, when using a voltage-mode approach in BB and a power mixer as in [4], [5], a V-I converter is required just before the up-converter. The noise of the V-I converter and that of the preceding block is not filtered. Therefore, to lower out-of-band noise, the power consumption of the BB stages is usually scaled-up toward the mixer. Moving the main filter in the last stage of the chain makes the noise of the preceding stages negligible making this solution potentially better than the one described in [4], [5] for out-of-band noise while saving some power.

The new filtering stage becomes the main noise contributor of the TX. However, since it is derived from the V-I converter of [4], its noise (which was already minimized and accounted for) remains practically unchanged. Indeed, the OTA and R_1 (Fig. 2-b) inject the same out-of-band noise as before, while R_2, the only noisy element added, has a low-pass transfer function to the output and does not contribute significantly to the overall output noise.

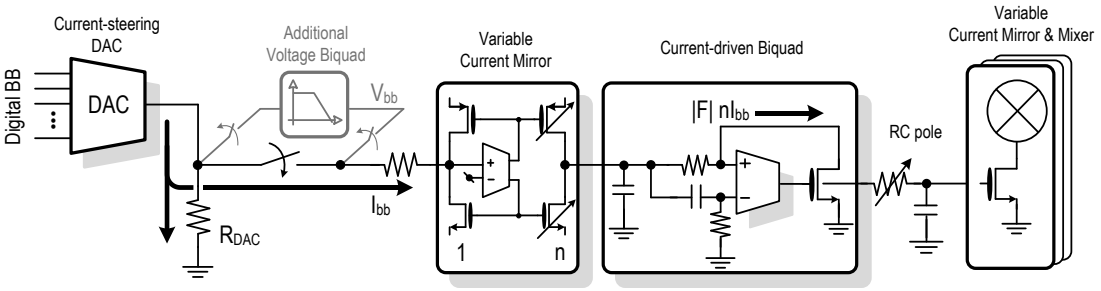

Fig. 3. Complete transmitter chain (single-ended version, I-path only)

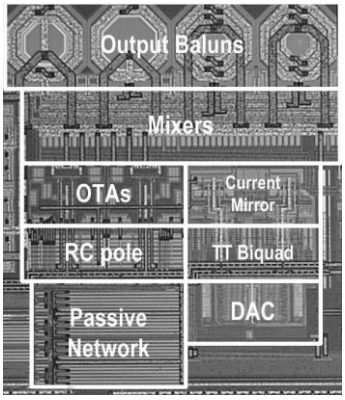

Fig. 4. Chip microphotograph

III. TRANSMITTER IMPLEMENTATION

The current-mode transmitter was implemented in a 55nm CMOS technology and tailored to 4G applications. A block diagram of the entire TX chain (I path-only) is shown in Fig. 3. To verify its advantages, the new solution was realized modifying the previous voltage-mode BB [4] while keeping the same DAC and the same class A/B power mixer.

To be compatible with the voltage output DAC and to be able to insert in the chain (for some critical standards) an additional biquad (as it is done in the previous design [4]), a V-I converter after the DAC is required. This is done putting a resistor in series to the variable-gain mirror input which behaves as a virtual ground thanks to the large loop gain of the OTA. The variable mirror feeds the filtering class A/B conditioner that realizes a 3rd order low-pass filter thanks to the additional real pole that was already present in the final mirror. Finally, the output current is up-converted via the class A/B power mixer that delivers power to different baluns, according to the transmission band [4].

The full transmitter features either a 3rd or a 5th order Butterworth filter depending on the selectivity required for coexistence with other wireless standard. In both cases, reconfigurability (as a function of the target standard) of the cut-off frequency is implemented. For the former case, the entire chain is operated in class A/B, leading to high efficiency. This is not the case when a 5th order filter is used. However, acting on the DAC oversampling (at very little cost in scaled-down technologies) it should be possible to use the fully class A/B (3rd order) chain for all cases with a further benefit in power consumption and out-of-band noise. Finally, in-band gain control is implemented changing the geometric factor of the current mirrors.

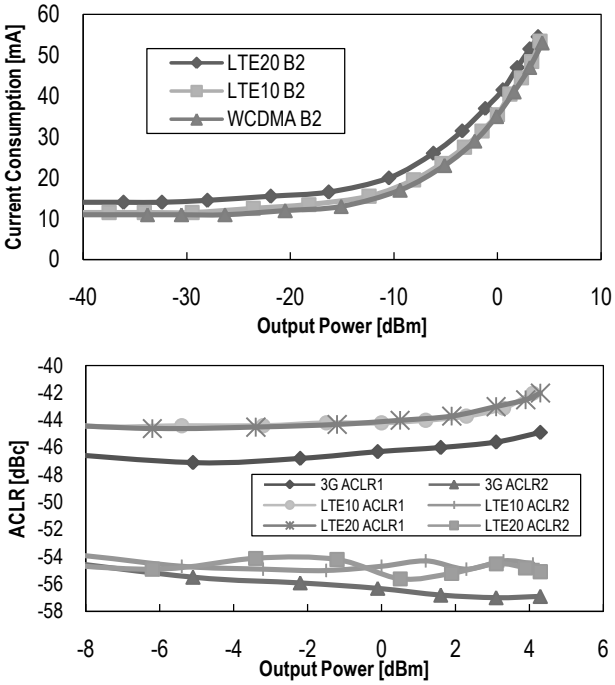

Fig. 5. TX current consumption and ACLR for 3G and 4G in Band2

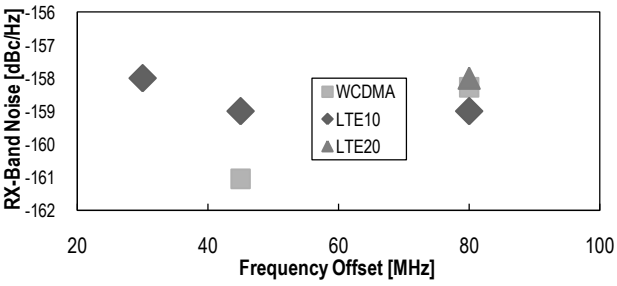

Fig. 6. RX-band noise for 3G and 4G

IV. MEASUREMENT RESULTS AND COMPARISONS

The chip active area is 1.5mm^2, dominated by the integrated baluns, and the microphotograph is shown in Fig. 4.

Fig. 5 shows the current drawn from the 1.8V supply for the entire chain (excluding DAC) versus transmitted power in Band2 for 3G and 4G (LTE10 and LTE20). This is almost independent of the standard and at low power (below -10dBm) is always less than 20mA. The difference between 3G or LTE10 and LTE20 is due to a larger OTA current, required to drive the last RC passive filter when its pole is tuned.

TABLE II. COMPARISON WITH VOLTAGE-MODE TXS

Parameter	Units	[2]			this work		
Standard	-	LTE10	LTE10	LTE20	LTE10	LTE10	LTE20
Band	-	5	12	2	5	17	2
Output Power	dBm	2.45	0.4	2.6	2.8	0.2	3.1
ACLR E-UTRA1/2 @Output Power	dBc	-41.4 -63	-41 -67	-38.4 -59	-43.4 -54.9	-44 -57.4	-43 -54.5
EVM @Output Power	%	1.7	1.9	2.4	1.4	1.4	1.4
Consumption @Output Power	mW	111.2	101.2	126.4	97	90	93
RX-band Noise @Output Power (frequency offset)	dBc/ Hz	-160.5[a] (45M)	-159[a] (30M)	-162.5[a] (80M)	-159[b] (45M)	-158[b] (30M)	-158[c] (80M)
Supply Voltage	V		1.1/2.5			1.8	
Chip Area	mm^2		0.98			1.06[d]	
CMOS Technology	nm		40			55 LP	

(a) Carrier-to-Noise ratio; (b) measured with 20 RB; (c) measured with 50 RB; (d) without DAC, TT Biquad and 2 baluns

TABLE I. COMPARISON WITH CURRENT-MODE TXS

Parameter	Units	[5]	[4]	this work	[5]	[4]	this work
Standard	-	LTE10			LTE20		
Max Output Power	dBm	3.7	6	6	4	6	6
Output Power	dBm	3.7	4	4	4	4	4
ACLR E-UTRA1/2 @4dBm	dBc	-40.3 NA	-44 -55	-42 -54.5	-40.3 NA	-40.9 -55	-42.5 -54.8
EVM HB (LB) @0 dBm	%	0.66 (NA)	1.8 (1.4)	1.8 (1.4)	1.05 (NA)	1.4 (1)	1.4 (1)
Consumption @4 dBm	mW	186	101	96	199	101	98
Consumption @-10 dBm	mW	56	39.5[a]	34	70	39.5[a]	36
RX-Band Noise (frequency offset)	dBc/ Hz	-155 (30M)	-154 (30M)	-158 (30M)	-157 (120M)	-155 (80M)	-158 (80M)
Supply Voltage	V	1.55/2.7	1.8	1.8	1.55/2.7	1.8	1.8
Chip Area	mm^2	5.06	1.3	1.5	5.06	1.3	1.5
CMOS Technology	nm	90	55 LP		90	55 LP	

(a) ISSCC 2013 Visual Supplement [4]

Fig. 5 also shows ACLRs measurements for 3G, LTE10 and LTE20 for Band2 for the left-side of the RF signal, which has a worse behavior than the right-side. $ACLR_{E\text{-}UTRA1}$ and $ACLR_1$ stay below -42dBc and -45dBc (for 4G and 3G) up to 4dBm. At low power the linearity is limited by the baseband, while at higher power by signal compression in the up-converter.

RX-band noise measurements for 4G standard have been made with transmitted signals composed of partial Resource Block (RB), as specified by 3GPP, while in the 3G case the full signal was used. The TX output was fed to the antenna port of a duplexer tuned to the target band and measurements were done on the RX port (with the TX port terminated on 50Ω), de-embedding the duplexer and cable attenuations. In this way, the transmitted signal was sufficiently suppressed by the stop-band of the duplexer to make it possible to measure the RX-band noise without saturating the spectrum analyzer. The results for the bands with the most critical TX-RX offsets are reported in Fig. 6, at 0dBm output power. The worst case is the LTE10 Band17, with a TX-RX offset of 30MHz, where the transmitter shows -158dBc/Hz.

A comparison with the state-of-the-art for 4G transmitters is given in Table I and Table II. Table I compares with a voltage-mode transmitter [2] for similar output powers and TX-RX offsets. Our solution shows better $ACLR_{E\text{-}UTRA1}$ and less power consumption and, featuring only one (at 1.8V) supply as opposed to two (at 1.1V and 2.5V), is less costly. RX-band noise is generally a bit larger for our implementation. However, in [2] the noise testing condition used (1MHz baseband tone [9]) is not 3GPP compliant and can give significantly better results. Chip area is less than 10% larger in our implementation, but using an older technology.

Table II compares with two recent current-mode transmitters. Compared to [4], our solution shows an improvement of 4dB in LTE10 and 3dB in LTE20 in the RX-band noise and requires, respectively, about 3mA and 2mA less current thanks to the new BB. In LTE10, the corresponding improvement, although very small at 4dBm, is already about 16% at -10dBm and exceeds 25% at very low output power. On the other hand, area is increased by about 15%.

Compared to [5], we have better RX-band noise and ACLR, worse EVM with a drastic power consumption (especially at high output power) and area reduction. Finally, also in this case the use of a single supply as opposed to two reduces costs.

ACKNOWLEDGMENT

The authors want to thank Marvell for technology access and Marvell Italy and Aliso Viejo (USA) Mobile Transceiver groups for help, support and fruitful discussions. This work was supported by the European M. Curie Grant N° 251399.

REFERENCES

[1] Xin He; Van Sinderen, J., "A 45nm low-power SAW-less WCDMA transmit modulator using direct quadrature voltage modulation," *Solid-State Circuits Conference - Digest of Technical Papers, 2009. ISSCC 2009. IEEE International* , vol., no., pp.120,121,121a, 8-12 Feb. 2009.

[2] Giannini, V. et al., "A multiband LTE SAW-less modulator with −160dBc/Hz RX-band noise in 40nm LP CMOS," *Solid-State Circuits Conference Digest of Technical Papers (ISSCC), 2011 IEEE International* , vol., no., pp.374,376, 20-24 Feb. 2011.

[3] S. Kousai and A. Hajimiri, "An Octave-Range, Watt-Level, Fully-Integrated CMOS Switching Power Mixer Array for Linearization and Back-Off-Efficiency Improvement," *Solid-State Circuits, IEEE Journal of* , vol. 44, no. 12, pp. 3376–3392, 2009.

[4] Rossi, P. et al., "An LTE Transmitter Using a Class-A/B Power Mixer", *Solid-State Circuits Conference Digest of Technical Papers (ISSCC), 2013 IEEE International* , vol., no., pp.340,342, Feb. 2013.

[5] Oliaei, O. et al., "A multiband multimode transmitter without driver amplifier," *Solid-State Circuits Conference Digest of Technical Papers (ISSCC), 2012 IEEE International* , vol., no., pp.164,166, 19-23 Feb. 2012.

[6] Sacchi, E.; Bietti, I.; Erba, S.; Tee, L.; Vilmercati, P.; Castello, R., "A 15 mW, 70 kHz 1/f corner direct conversion CMOS receiver," *Custom Integrated Circuits Conference, 2003. Proceedings of the IEEE 2003* , vol., no., pp.459,462, 21-24 Sept. 2000.

[7] Hogervorst, Ron; Tero, John P.; Eschauzier, Ruud G H; Huijsing, J.H., "A compact power-efficient 3 V CMOS rail-to-rail input/output operational amplifier for VLSI cell libraries," *Solid-State Circuits, IEEE Journal of* , vol.29, no.12, pp.1505,1513, Dec 1994.

[8] Cassia, M. et al., "A Low-Power CMOS SAW-Less Quad Band WCDMA/HSPA/HSPA+/1X/EGPRS Transmitter," *Solid-State Circuits, IEEE Journal of* , vol.44, no.7, pp.1897,1906, July 2009.

[9] Craninckx, J.; Borremans, J.; Ingels, M., "SAW-less software-defined radio transceivers in 40nm CMOS," *Custom Integrated Circuits Conference (CICC), 2011 IEEE* , vol., no., pp.1,8, 19-21 Sept. 2011.